Article

Chemistry & Biology

# Non-canonical Bromodomain within DNA-PKcs Promotes DNA Damage Response and Radioresistance through Recognizing an IR-Induced Acetyl-Lysine on H2AX

## Graphical Abstract

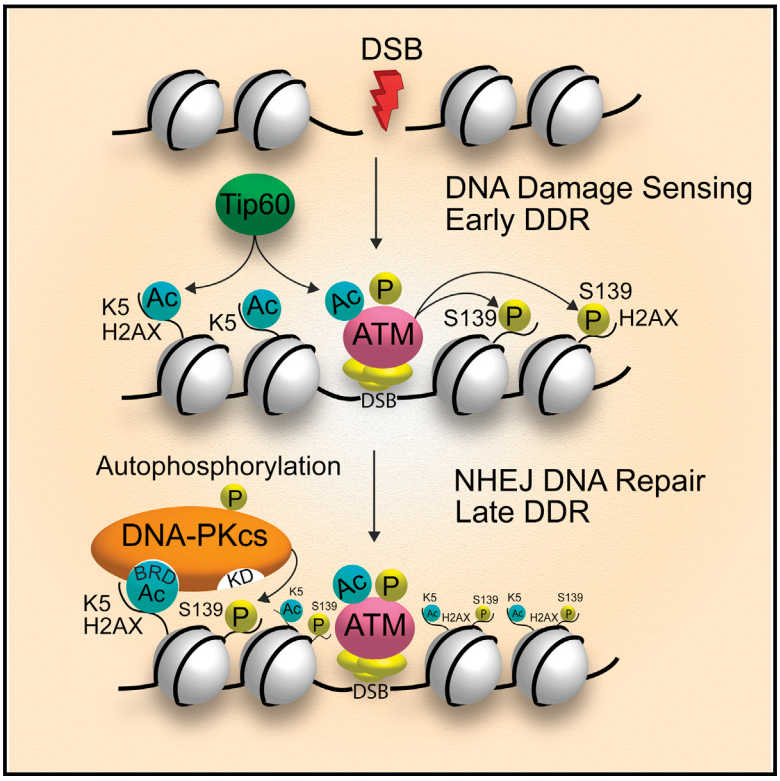


## Highlights

- Top-down mass spec reveals IR-induced concerted increases of K5ac and phospho-H2AX
- A bromodomain module was found in DNA-PKcs to recognize the acetyl-lysine 5 on H2AX
- The DNA-PKcs-BRD defines the activity of DNA-PKcs to phosphorylate Ser139 on H2AX
- DNA-PKcs activity in NHEJ repair is K5ac dependent and contributes to radioresistance

## Authors

Li Wang, Ling Xie, Srinivas Ramachandran, ..., Jian Jin, Nikolay V. Dokholyan, Xian Chen

## Correspondence (main)

xianc@email.unc.edu (X.C.)

## Co-correspondence (molecular modeling)

dokh@unc.edu (N.V.D.)

## In Brief

DNA-dependent protein kinase catalytic subunit (DNA-PKcs) is a major kinase involved in DNA repair and V(D)J recombination. Wang et al. discover a bromodomain (BRD)-like module in DNA-PKcs that recognizes H2AX acetyl-lysine 5, and present evidence that this interaction is critical for H2AX-dependent regulation of DNA-PKcs in IR-induced, differential DNA damage response.

Wang et al., 2015, Chemistry & Biology 22, 849–861
July 23, 2015 
http://dx.doi.org/10.1016/j.chembiol.2015.05.014

Chemistry & Biology
Article

# Non-canonical Bromodomain within DNA-PKcs Promotes DNA Damage Response and Radioresistance through Recognizing an IR-Induced Acetyl-Lysine on H2AX

Li Wang,[1,2] Ling Xie,[2] Srinivas Ramachandran,[2,3] YuanYu Lee,[2] Zhen Yan,[2,5] Li Zhou,[2] Krzysztof Krajewski,[2] Feng Liu,[4,7] Cheng Zhu,[2] David J. Chen,[8] Brian D. Strahl,[2] Jian Jin,[6] Nikolay V. Dokholyan,[2,3,4,**] and Xian Chen[1,2,3,4,*]
[1]Department of Chemistry & Institutes of Biomedical Sciences, Fudan University, Shanghai 20032, China
[2]Department of Biochemistry & Biophysics, University of North Carolina at Chapel Hill, Chapel Hill, NC 27599, USA
[3]Program in Molecular & Cellular Biophysics, University of North Carolina at Chapel Hill, Chapel Hill, NC 27599, USA
[4]Lineberger Comprehensive Cancer Center, University of North Carolina at Chapel Hill, Chapel Hill, NC 27599, USA
[5]College of Public Health, Zhengzhou University, Zhengzhou 450001, China
[6]Departments of Structural and Chemical Biology, Icahn School of Medicine at Mount Sinai, NY 10029, USA
[7]Department of Medicinal Chemistry, Soochow University, Suzhou 215123, China
[8]Department of Radiation Oncology, UT Southwestern Medical Center, Dallas, TX 75390, USA
*Correspondence (main): xianc@email.unc.edu (X.C.)
**Co-correspondence (molecular modeling): dokh@unc.edu (N.V.D.)
http://dx.doi.org/10.1016/j.chembiol.2015.05.014

## SUMMARY

**Regulatory mechanisms underlying γH2AX induction and the associated cell fate decision during DNA damage response (DDR) remain obscure. Here, we discover a bromodomain (BRD)-like module in DNA-PKcs (DNA-PKcs-BRD) that specifically recognizes H2AX acetyl-lysine 5 (K5ac) for sequential induction of γH2AX and concurrent cell fate decision(s). First, top-down mass spectrometry of radiation-phenotypic, full-length H2AX revealed a radiation-inducible, K5ac-dependent induction of γH2AX. Combined approaches of sequence-structure modeling/docking, site-directed mutagenesis, and biochemical experiments illustrated that through docking on H2AX K5ac, this non-canonical BRD determines not only the H2AX-targeting activity of DNA-PKcs but also the over-activation of DNA-PKcs in radioresistant tumor cells, whereas a Kac antagonist, JQ1, was able to bind to DNA-PKcs-BRD, leading to re-sensitization of tumor cells to radiation. This study elucidates the mechanism underlying the H2AX-dependent regulation of DNA-PKcs in ionizing radiation-induced, differential DDR, and derives an unconventional, non-catalytic domain target in DNA-PKs for overcoming resistance during cancer radiotherapy.**

## INTRODUCTION

Based on the severity of DNA double-stranded breaks (DSBs) and the duration of stress exposure, cells take different decision-making pathways toward either apoptosis or survival (Lobrich and Jeggo, 2007). An acute ionizing radiation (IR) usually triggers pro-apoptotic signals in cells with irreparable DSBs or active DNA repair of surviving cells, whereas cells constantly exposed to lower radiation doses can become tolerant or adapted to the frequent DNA damage caused by repeated irradiation (Mullenders et al., 2009). Cells with such an adaptive response are generally discerned by reduced sensitivity to stimuli, as tumor cells can escape immunosurveillance under IR-adaptive conditions, contributing to an increased risk of chronic inflammation-associated carcinogenesis and acquired radioresistance in tumor cells (Mullenders et al., 2009).

As one of the earliest cellular DNA damage responses (DDR), a replacement histone variant, H2AX, senses DSBs through rapid phosphorylation of the highly conserved Ser139 (Bonner et al., 2008). This phosphorylation at Ser139, or γH2AX, then serves as a central scaffold that recruits protein factors associated with diverse functions including IR-induced cell-cycle arrest (Du et al., 2006) and nucleosome dynamics (Heo et al., 2008), resulting in γH2AX foci over large chromatin domains surrounding DSBs (van Attikum and Gasser, 2009). Although evidence indicates the central role of DSB-inducible γH2AX in coordinating diverse processes of DSB repair and cell fate decision (Bonner et al., 2008), exactly how the phenotypic regulation of γH2AX is achieved, and its impact on either normal or abnormal cell fate decision, is still obscure.

As one of the two H2AX-targeting kinases that play a redundant role in regulating γH2AX, DNA-dependent protein kinase catalytic subunit (DNA-PKcs) not only promotes the H2AX-mediated apoptosis or DNA repair of damaged cells, but also, when over-activated, contributes to the resistance to DSB-induced apoptosis in human malignant cells (Deriano et al., 2005). These observations immediately raise the mechanistic questions as to how DNA-PKcs regulates these totally opposite DDRs. Based on a previous report that phosphorylation of H2AX by DNA-PK could be stimulated only in the context of acetylation-rich nucleosomes (Park et al., 2003), we reason that there could be an

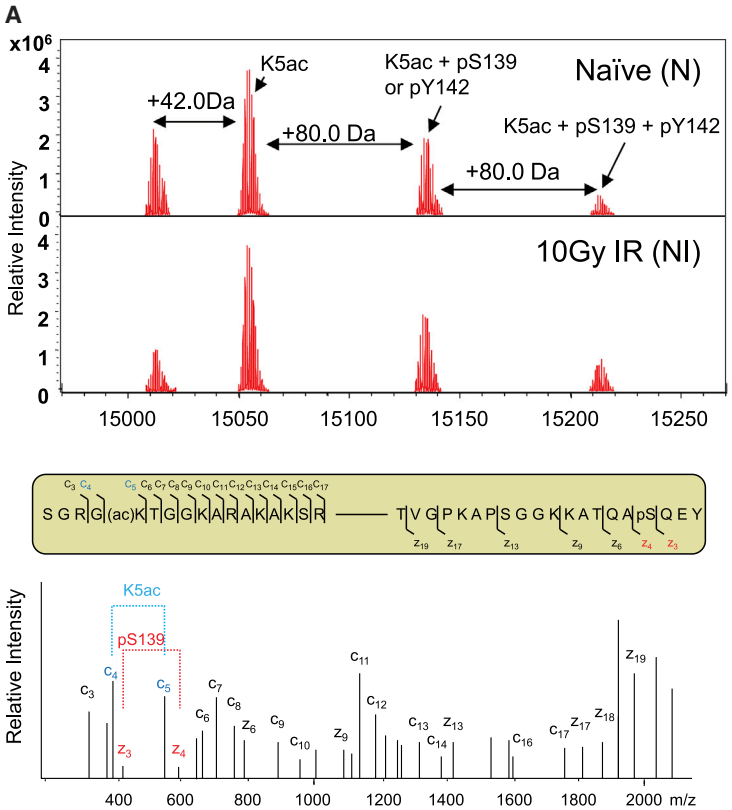


| H2AX PTMs | Relative Abundance, % | |
|---|---|---|
| | N | NI |
| Unmodified | 25.8 | 14.4 |
| K5ac | 44.1 | 49.1 |
| K5ac + P | 23.7 | 25.1 |
| K5ac + 2P | 6.5 | 11.4 |
| K5ac + $P_{total}$ | 30.2 | 36.5 |

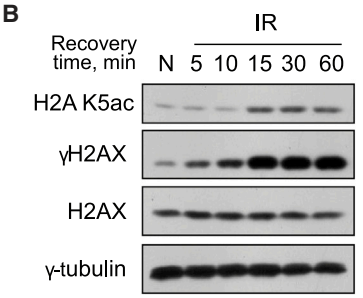


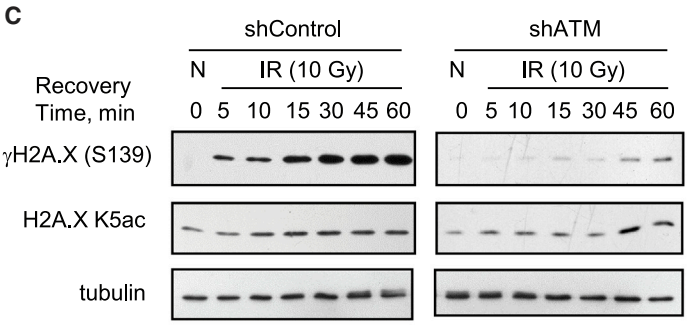


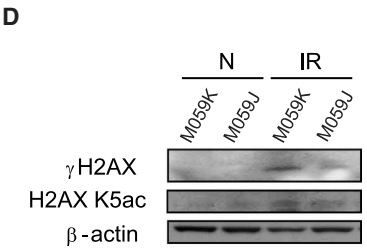


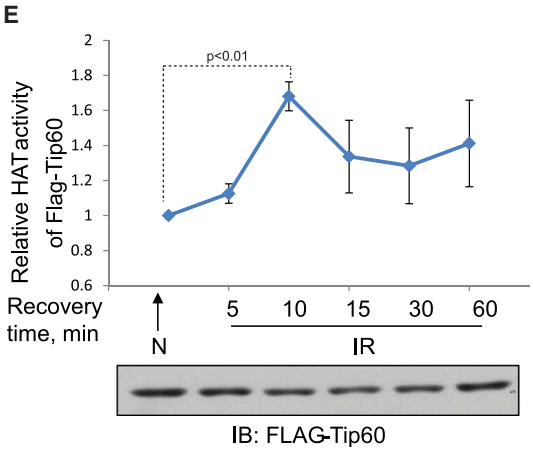


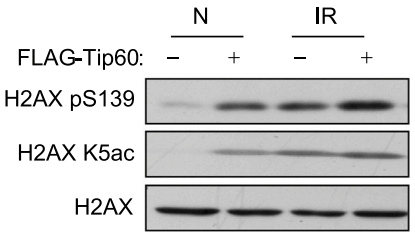


(legend on next page)

acetylation-dependent mechanism underlying the activation of DNA-PKcs during H2AX-mediated DDR.

Given the cross-regulations that exist among different post-translational modifications (PTMs) on H2AX for either apoptosis or survival (Cook et al., 2009) or chromatin reorganization during DDR (Ikura et al., 2007), we first mapped the combinatorial PTM pattern on H2AX and its IR-induced changes by using 12-T Fourier transform ion cyclotron resonance (FTICR) mass spectrometry (MS) with ultra-high mass accuracy and resolution, whereby we simultaneously identified multiple acetyl-lysines (Kac) in a full-length protein so that their relative abundances were quantified (Zhao et al., 2010). As a result, we observed an IR-inducible, concerted increase in both acetylated lysine 5 (K5ac) and γH2AX. Furthermore we found that, in the later phase of IR-induced DDR and in a K5ac-dependent manner, DNA-PKcs was the primary kinase to phosphorylate H2AX Ser139. A combined approach utilizing molecular modeling/docking, site-directed mutagenesis, and biochemical/cell biology analyses revealed a novel bromodomain (BRD)-like module in DNA-PKcs that not only specifically recognizes K5ac on H2AX but also tightly binds to JQ1, a small-molecule antagonist of bromodomain and extra terminal (BET) BRD and a Kac-structure mimic (Filippakopoulos et al., 2010). Furthermore, we found that the DNA-PKcs activity for inducing γH2AX is K5ac/BRD dependent, and that this K5ac-dependent activity of DNA-PKcs acts as a double-edged sword, promoting either the DDR of acutely irradiated cells or the radioresistance of chronically irradiated cells. We mechanistically reveal that the K5ac induced on H2AX by prior irradiation is responsible for the early phase over-activation of DNA-PKcs in radioresistant leukemia cells (Deriano et al., 2005) where DNA-PKcs-BRD recognizes the H2AX K5ac during the activation of DNA-PKcs for non-homologous end-joining (NHEJ) repair. Unlike most of the available drugs targeting the catalytic domain of DNA-PKcs (Bruce et al., 2012), our findings indicate a novel NHEJ pathway-specific, unconventional target of (+)-JQ1 that could re-adjust the imbalanced activity of DNA-PKcs in the H2AX-mediated NHEJ. As an immediate result of (+)-JQ1 pre-treatment, the mitochondria-mediated apoptotic pathway was found to be re-activated in the radioresistant leukemia cells that regained sensitivity to IR.

## RESULTS

### The IR-Inducible γ-Ser139 on H2AX Could Be K5ac Dependent

We first performed FTICR MS and electron capture dissociation (ECD) tandem MS (MS/MS) (Zhao et al., 2010) to examine if 10 Gy IR could induce any concerted changes in different PTMs on H2AX. We purified by high-performance liquid chromatography (HPLC) the histones extracted from 10 Gy-irradiated cells following a 1-hr post-irradiation recovery, and used FTICR MS to analyze the single species in fraction 19 (Figure S1A). From low to high *m/z*, three different forms of full-length H2AX were MS/MS-sequenced and identified in a combinatorial manner as the following: unmodified H2AX, H2AX K5ac, K5ac with γ-Ser139, and K5ac with both γ-Ser139 and γ-Tyr142 (Figure 1A; Figures S1B–S1E).

Notably, in this particular HPLC fraction (Figure S1A) the acetylated forms of H2AX that have sufficient amounts for unambiguous MS/MS sequencing were found as the dominant species, while the population of non-acetylated H2AX was minor or could be suppressed during MS analysis so that no γ-Ser139 was detected on the unacetylated form of H2AX. Also, although a minor population of putative ubiquitinated H2AX was detected by MS, it was too weak to be sequenced by ECD MS/MS.

Because of simultaneous identification of both PTMs on full-length H2AX, we were able to quantitatively analyze IR-induced, concerted changes in multiply modified H2AX (Figure 1A): Following high-dose IR and 1-hr recovery, the relative amount of unphosphorylated form in the total acetylated H2AX population was reduced by approximately 50%, from 25.8% to 14.4% (see table in Figure 1A). Meanwhile, the increases of both single and double phosphorylations (γ-Ser139 or and γ-Tyr142) occurred only on the K5ac form of H2AX, and both K5ac and γ-Ser139 or/and γ-Tyr142 were simultaneously increased compared with non-irradiated cells, indicating that both acetylation and phosphorylations on H2AX are coupled

**Figure 1. IR-Inducible Phosphorylation of γ-Serine 139 on H2AX Could Be K5ac Dependent**

(A) (Top) Top-down micro-electrospray ionization FTICR MS analysis of full-length H2AX isolated from non-irradiated or 10 Gy-irradiated cells. +42 Da or +80 Da corresponds to addition of an acetyl or a phosphate group. Each mass spectrum was acquired in the ICR cell with 100 scans. (Middle) Sequence locations of ECD MS/MS fragment ions detected at either the N terminus (c ions) and C terminus (z ions) on modified H2AX. (Bottom) ECD MS/MS spectra of the H2AX precursor ions at *m/z* 1,513.62 Da with 10+ charges, showing the fragment ions for K5ac and γ-Ser139. N-terminal (c ions) and C-terminal (z ions) fragment ions indicating the corresponding PTM are marked in red and blue, respectively. The ECD MS/MS spectrum shown with the low *m/z* fragment ions corresponds to N-terminal K5ac and C-terminal γ-Ser139.

(B) Immunoblot analysis of 10 Gy IR-induced time-dependent changes of K5ac or γ-Ser139. Non-irradiated or 10 Gy-irradiated (100 rad/min for 10 min) HeLa cells were collected at 5, 10, 15, 30, and 60 min after IR. Cells were lysed with 200 μl of SDS sample buffer, and 5 μl was separated on 15% SDS-PAGE, transferred to polyvinylidene fluoride, and probed with the antibody against either γH2AX or H2A K5ac.

(C) Immunoblot analysis of 10 Gy IR-induced time-dependent changes of K5ac or γ-Ser139 in the wild-type F1-hTERT-shLacZ (control) versus ATM KD F1-hTERT-shATM cells.

(D) DNA-PKcs directly contributes to the high-dose IR-induced γH2AX in the later phase of DDR. Both M059K and M059J DNA-PKcs-deficient human glioma cell lines were irradiated by a 10 Gy IR and allowed to recover for 60 min. β-Actin was used as the loading control. Quantitative analysis of the changes of K5ac or γ-Ser139 was performed as described in the Experimental Procedures. One experimental point containing three technical duplicates representative of two is shown, with the data precision indicated by the error bar based on mean ± SD of duplicate samples.

(E) 10 Gy IR-induced time-dependent changes in the activity of Tip60. 293T cells were transfected with FLAG-Tip60, irradiated by 10 Gy IR, and harvested at each indicated time. Tip60 was immunoprecipitated using anti-flag antibody from the non-irradiated or irradiated cells collected at each recovery time, and its time-dependent HAT activity was determined using a colorimetric assay (BioVision) and normalized against the amount of FLAG-Tip60 determined by immunoblot.

(F) Exogenous Tip60 triggered greater simultaneous increases of K5ac and γ-Ser139 on H2AX in non-irradiated HeLa cells. HeLa cells without or with FLAG-Tip60 transfection were subjected to radiation and immunoblotting with indicated antibody. H2AX was used as the loading control.

under a high dose of IR. Our discovery-driven, phenotype-specific, top-down MS analysis thus indicated that these H2AX PTMs are coordinately deposited during IR-induced DDR. Due to the *m/z* degeneracy between γ-Ser139 and γ-Tyr142, the proportion of these two phosphorylated forms was not distinguishable in MS spectra. We therefore used immunoblotting to determine which one of γ-Ser139 or γ-Tyr142, or both, contributes to the IR-inducible abundance changes. First, we verified the K5ac dependence of the DSB-induced site-specific phosphorylation(s) in different cell types after exposure to IR at different dose levels. In agreement with our FTICR MS results (Figure 1A), both K5ac and γ-Ser139 showed the same trend of simultaneous increase with increasing doses of IR, while γ-Tyr142 showed little IR-inducible change (Figure S2A), further indicating that the majority of the observed IR-inducible, K5ac-dependent increases of phosphorylation is from γ-Ser139. Results from IR-phenotypic screening of H2AX PTMs by using both top-down MS and immunoblotting then generated the central hypothesis that γ-Ser139 may be induced by high-dose acute IR in a Kac-dependent manner.

## DNA-PKcs Is the K5ac-Dependent Kinase that Phosphorylates Serine 139

We then searched for a K5ac-dependent, H2AX-targeting kinase, and clarified the biological implications of its K5ac dependence. Previous work indicated that Ser139 phosphorylation was still inducible by 10 Gy IR on a K5R H2AX mutant (Xie et al., 2010), suggesting that not all phosphatidylinositol-3-kinase-related (PIKK) family kinases for Ser139 phosphorylation, including ataxia telangiectasia mutated (ATM) and DNA-PK (Bonner et al., 2008), function in a Kac-dependent manner. First, we investigated exactly how IR-induced changes of γ-Ser139 and K5ac are coordinated in 10 Gy-irradiated cells collected at different post-irradiation times. In HeLa cells, within the first 10 min of recovery following high-dose IR, γ-Ser139 increased whereas K5ac remained at its basal level (Figure 1B). After 15 min, however, both K5ac and γ-Ser139 increased significantly, indicating that the K5ac dependence on Ser139 phosphorylation occurs only in irradiated cells with longer post-irradiation recovery. Furthermore, to determine when ATM plays a dominant role in Ser139 phosphorylation, we compared the IR-induced, time-resolved changes of both PTMs in a pair of ATM knock-down (KD) cells, F1-hTERT-shATM (ATM KD), with a wild-type (WT) control, F1-hTERT-shLacZ (Heffernan et al., 2002). While WT cells showed time-dependent changes similar to those in HeLa cells (Figure 1C, left), shRNA-mediated ATM KD led to diminished γ-Ser139 at an early stage of post-irradiation recovery. However, later simultaneous increases of both K5ac and γ-Ser139 were unaffected by ATM KD (Figure 1C, right), indicating that, during the early phase of DDR, ATM is the primary kinase targeting H2AX in a K5ac-independent manner.

DNA-PKcs, therefore, became the likely kinase responsible for the later increase of γ-Ser139, which is accompanied by an increase in K5ac. To confirm this, we first examined the IR-induced changes of γ-Ser139 and K5ac during the late phase of DDR on a pair of human glioma cell lines, M059K (WT DNA-PKcs) and M059J (DNA-PKcs deficient) (Lees-Miller et al., 1995). Simultaneous increases of K5ac and γ-Ser139 in irradiated cells with a recovery longer than 15 min were observed only in WT cells but not in the DNA-PKcs-deficient cells (Figure 1D). Although a low level of ATM expression was found in M059J cells (Fang et al., 2012), these DNA-PKcs-deficient cells clearly showed a lack of IR-inducible, coordinated increase in K5ac and γ-Ser139. Furthermore, the composition of the 10 Gy IR-induced H2AX-interactome recently dissected by our multiplex quantitative proteomics indicated enhanced interactions between H2AX and the DNA-PK complex (Lee et al., 2012) coincident with the high-dose IR-induced increase of K5ac, also supporting that DNA-PKcs is the primary H2AX-targeting kinase at 1 hr post-IR recovery, which correlated with the defined H2AX PTM pattern (Figure 1A).

We then clarified the sequential order of depositing these PTMs on H2AX by examining the effect of a K5ac-targeting histone acetyltransferase (HAT), Tip60 (Sun et al., 2007), on the level of γ-Ser139. First, the HAT activity of Tip60 showed a trend of changes similar to that of either K5ac or γ-Ser139 in the 10 Gy-irradiated cells during the same period of post-IR recovery (Figure 1E), implicating the IR-inducible Tip60 activity in depositing K5ac. Furthermore, in non-irradiated cells with a low level of K5ac, over-expression of Tip60 led to dramatic increases in both K5ac and γ-Ser139 (Figure 1F). Notably, over-expression of exogenous Tip60 contributed little to the already high level of K5ac in 10 Gy-irradiated cells, suggesting that, compared with non-irradiated cells, endogenous Tip60 in IR-responsive cells was fully activated by high-dose IR to acetylate H2AX. However, the low activity of endogenous Tip60 in non-irradiated cells was supplemented by over-expressed Tip60, resulting in higher K5 acetylation. These results indicated that the IR-inducible, Tip60-promoted K5 acetylation is a prerequisite for Ser139 phosphorylation, and recognition of H2AX by DNA-PK is enhanced due to more K5ac during the later DDR phase when the activity of DNA-PKcs depends on acetylated H2AX.

## DNA-PKcs Contains a BRD-like Structural Module to Recognize H2AX K5ac

We next investigated the structural basis for the K5ac-dependent activation of DNA-PKcs. Based on the DNA-PK crystal structure (Sibanda et al., 2010), we used a sequence-structure modeling approach to explore whether any region in DNA-PKcs shares structural homology with BRDs. The crystal structure of DNA-PKcs features various regions named head, forehead, putative DNA-binding domain, and ring structure (Sibanda et al., 2010) (PDB: 3KGV; Berman et al., 2000). However, due to low resolution (6.6 Å), only the protein backbone forming different secondary structural elements was discernible, whereas the identities of the residues in the corresponding structural regions were not known. Thus, we first used Situs (Wriggers, 2009) to align the structure of the catalytic N and C lobes of phosphoinositide 3-kinase (PI3K, PDB: 1E8X) onto the crystal structure of DNA-PKcs (Figure S3). The PI3K catalytic subunit aligned well with the head/crown region of DNA-PKcs (Figures 2A and 2B). Furthermore, using Situs we examined alignments of the previously determined BRD structures with the DNA-PKcs structure, and found significant structural homology between the BRD and a region of the HEAT repeats in the DNA-PKcs ring structure, which was confirmed using the Dali server (Holm and Rosenstrom, 2010) (Figures 2A and 2C; Table S1).

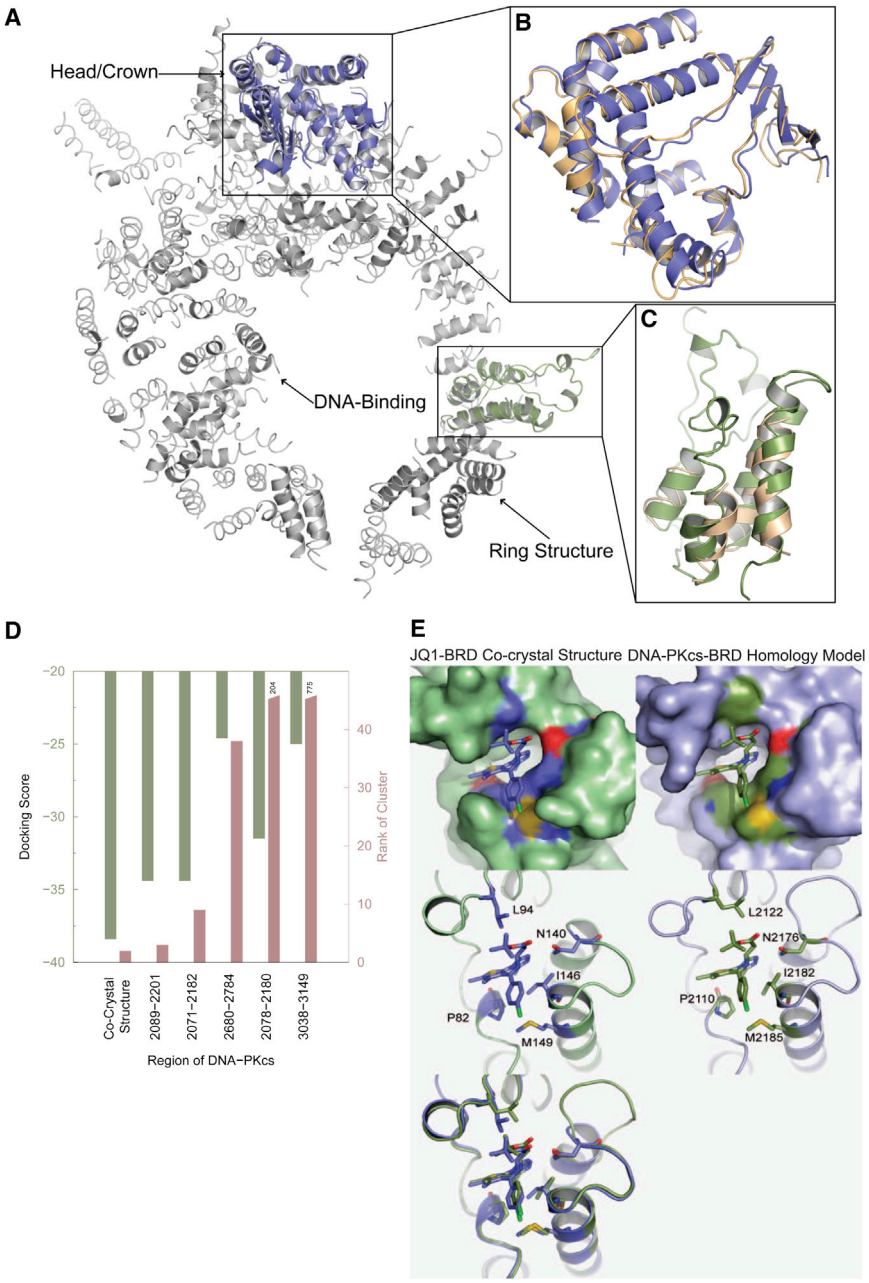


**Figure 2. Molecular Modeling/Docking Reveals a Kac-Recognizing, BRD-like Structure in DNA-PKcs**

(A) Structural alignment of DNA-PKcs (gray) with the catalytic subunit of PI3K (blue) and the BRD template (green).

(B) Detailed structural alignment of PI3K catalytic subunit (blue) with DNA-PKcs (orange).

(C) Detailed structural alignment of the BRD (green) with DNA-PKcs (orange). Here, Dali reported a Ca root-mean-square deviation between BRD and the aligned region of DNA-PKcs to be 2.1 Å and a *Z* score of 5.1, both of which indicate statistically significant structural homology (Table S1). The structures are rendered in cartoon representation using PyMOL.

(D) Summary of docking results for different DNA-PKcs-BRD homology models. To select the best region that could form BRD in DNA-PKcs, docking studies were performed on all possible DNA-PKcs-BRD homology models. The docking score represents a combination of the stability of BRD-JQ1 complex and the strength of interaction of JQ1 with BRD. A negative docking score indicates better binding of JQ1 to BRD. The docking scores of the near-native poses are presented. The cluster rank illustrates the extent of sampling of the near-native poses. Top-ranked near-native clusters indicate better amenability of the BRD to bind JQ1. The co-crystal structure has the best docking score and cluster rank. Closest to the co-crystal structure is the putative BRD formed by residues 2,089–2,201 in DNA-PKcs.

(E) Near-native docked pose of DNA-PKcs-BRD homology model. (Top) Surface representation of the pocket binding JQ1 in mouse BRD4 co-crystal structure (left) and the DNA-PKcs-BRD homology model (right). The bound ligand (JQ1) is shown in stick representation. The surface of residues in the pocket that are identical between mouse BRD4 and DNA-PKcs-BRD are colored in contrast to the rest of the binding pocket (blue, yellow, and red in the co-crystal structure; green, yellow, dark blue, and red in the BRD homology model). (Middle) The binding poses are shown in the same view, but shown with cartoon representation to enable visualization of the positions of the residues in the binding pocket that are identical between mouse BRD4 and DNA-PKcs-BRD. These residues are shown as sticks and their positions in the corresponding sequences are labeled. (Bottom) The structural overlay of co-crystal structure and the BRD homology model further illustrates the similarities in the binding mode of JQ1 and the residues lining the binding pocket.

We then used a combination of sequence-structure alignment and molecular docking, MedusaDock (Ding et al., 2010), to identify the exact sequence and location of this BRD in DNA-PKcs. Using FUGUE, we threaded the DNA-PKcs sequence through representative crystal structures of BRDs to arrive at putative sequence-structure alignments that pinpointed BRD in several possible regions of DNA-PKcs (Table S2). To find the region that best represents a BRD, based on the co-crystal structure between BRD4(1) and an BET BRD-specific inhibitor (+)-JQ1 (Filippakopoulos et al., 2010), we constructed homology models of BRD4 using a sequence corresponding to all these regions, and ranked the JQ1 binding ability of the homology models using MedusaDock. Considering both the docking score of the near-native pose and the rank of the near-native cluster (Figure 2D), we found residues 2,089–2,201 to represent the best possible region to form a putative BRD4 in DNA-PKcs, as the alignment of DNA-PKcs with the crystal structure of mouse BRD4 (mBRD4, PDB: 3JVK) indicated a large similarity (59%) with the BRD-characteristic left-handed bundle of four α helices (Filippakopoulos et al., 2012), linked by loop regions of variable length

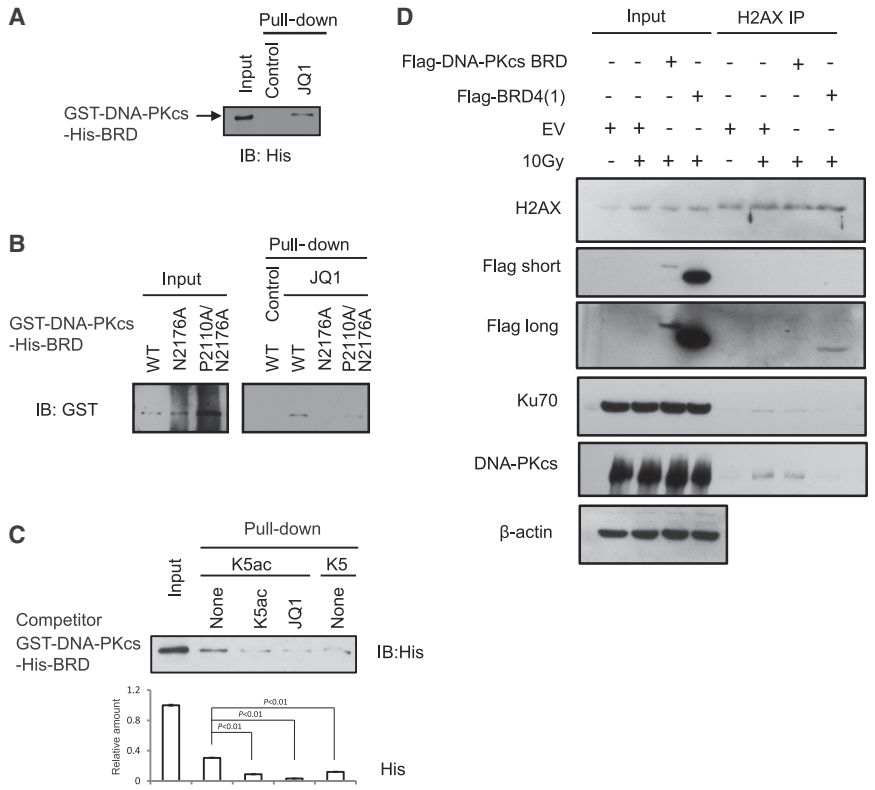


**Figure 3. The DNA-PKcs-BRD Specifically Recognizes H2AX K5ac**

(A and B) Immuoblot analysis of JQ1 binding to (A) the BRD-containing DNA-PKcs fragment (amino acids [aa] 1,878–2,700), and (B) the mutants of this DNA-PKcs-BRD fragment including a single mutant N2176A and a double mutant P2110A/N2176A. These proteins were purified under denaturing conditions and re-folded for the binding assay.

(C) Analysis of comparative binding between the DNA-PKcs-BRD and the peptides containing either K5ac or non-acetylated K5 peptide without or with 10 μM JQ1.

(D) Immunoblot analysis of the H2AX complexes pulled down, respectively, from the U2OS cells transfected with either empty vector (EV) or the vector containing either gene-expressing flag-tagged DNA-PKcs-BRD or flag-tagged BRD4(1). Some sets of the cells were irradiated by 10 Gy IR as indicated. The immunoprecipitates were blotted against the indicated antibody including DNA-PKcs, Ku70, or H2AX.

(Figure S4). Strikingly, the structural model formed by DNA-PKcs-BRD and JQ1 with the published BRD4-JQ1 co-crystal structure (Figure 2E, top; Figure S5) showed that many of the functionally significant residues in each Kac binding pocket were identical in their interactions with JQ1, e.g., the alignment re-capitulates a conserved asparagine (Owen et al., 2000) involved in Kac binding (N140 in mBRD4 versus N2176 in DNA-PKcs) (Figure 2E, middle), indicating a good shape complementarity between both structures of BRDs in their JQ1-binding pockets (Figure 2E, bottom).

To experimentally validate our docking modeling that derives the JQ1-bound DNA-PKcs-BRD, we expressed, purified, and re-folded epitope-tagged DNA-PKcs fragments (amino acids [aa] 1,878–2,700) comprising the putative BRD domain (aa 2,070–2,200). Two mutants of this DNA-PKcs-BRD fragment, a single mutant N2176A and a double mutant P2110A/N2176A, were also generated, based on their locations in the JQ1/Kac binding pocket (Figure 2E). First, we used circular dichroism to confirm that WT or mutants of DNA-PK-BRD are properly re-folded (Figure S6), and the WT DNA-PKcs-BRD fragment showed unambiguously specific binding to JQ1 when incubated with Sepharose-immobilized JQ1 (Figure 3A). Compared with WT DNA-PKcs, the binding of JQ1 to both mutants was weakened (even with higher amounts of protein loaded), particularly for the N-depleted mutant(s) (Figure 3B), validating the accuracy of our modeling the JQ1 binding pocket in DNA-PKcs that was disrupted by substitution of a key pocket asparagine present in most BRDs (Owen et al., 2000). The binding constants were not accessible at this point due to the instability of re-folded proteins.

To prove the specificity of DNA-PKcs-BRD in recognizing K5ac, we then compared binding between WT DNA-PKcs-BRD and H2AX peptides containing either unacetylated K5 or K5ac. In line with the result from a peptide array study of BRD binding in which the highly conserved N-terminal sequences of both H2A and H2AX strongly bound to BRD4 (Filippakopoulos et al., 2012), DNA-PKcs-BRD showed a stronger binding to the K5ac-containing peptide compared with its unacetylated counterpart (Figure 3C). Furthermore, the addition of JQ1, the tighter binder of BRD4, completely abolished binding between DNA-PKcs-BRD and K5ac, indicating that the DNA-PKcs-BRD is a BRD4-like structure for Kac recognition with which JQ1 can compete.

Because JQ1 is a BET BRD-specific inhibitor that affects the functions of various Kac-recognizing, BET/BRD-containing proteins in cells, we investigated whether DNA-PKcs-BRD is indeed the functional module specifically involved in the IR-induced interaction between the DNA-PK complex and H2AX. We then generated a vector expressing only the BRD region of DNA-PKcs-BRD (aa 2,070–2,200) with a size comparable with that of BRD4(1), and found that its specific binding to Kac-mimic JQ1 was preserved (Figure S7A). In the 10 Gy IR-induced, H2AX-associated complexes pulled down by H2AX antibody from, respectively, the U2OS cells transfected with either empty vector (EV) or DNA-PKcs-BRD or BRD4(1) prior to 10 Gy IR, we found that over-expression of either DNA-PKcs-BRD or BRD4(1) led to dissociation of endogenous DNA-PKcs from H2AX (Figure 3D). These results together indicate that the BRD of DNA-PKcs is the structural determinant for promoting the IR-induced interaction between the DNA-PK complex and H2AX; therefore, the exogenously expressed DNA-PKcs-BRD could disrupt IR-induced, BRD-dependent interaction between H2AX and the endogenous DNA-PKcs.

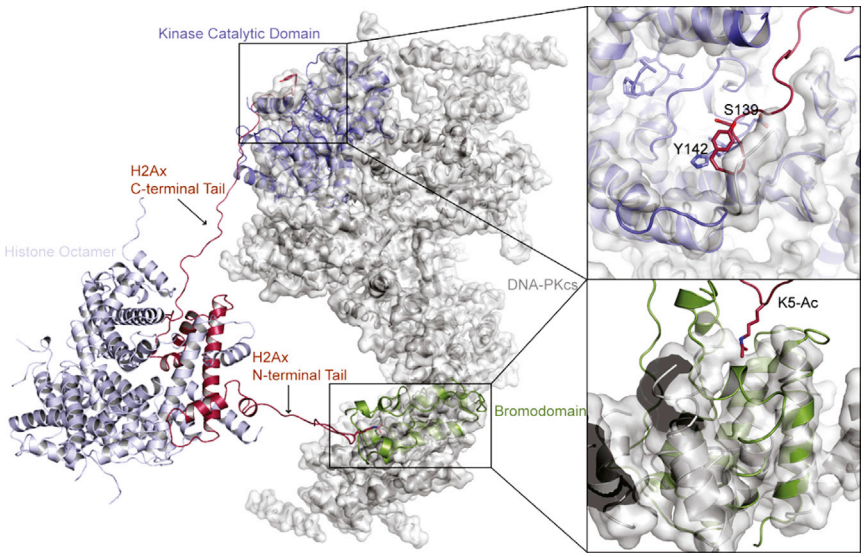


**Figure 4. Simultaneous Binding of an H2AX-Containing Nucleosome to the BRD and the Kinase Domain of DNA-PKcs**

A structural model of an H2AX-containing nucleosome, with the N-terminal tail of H2AX bound to the putative BRD of DNA-PKcs (through K5ac) and the C-terminal tail positioned in the catalytic region of the kinase domain of DNA-PKcs (which would facilitate phosphorylation of Ser139). The detailed binding modes of Ser139 and K5ac are shown on the right. DNA-PKcs is rendered in surface and cartoon representation, whereas the nucleosome is rendered in cartoon representation. K5ac, Ser139, and Tyr142 are rendered in stick representation. The PI3K catalytic subunit (blue) and the bromodomain template (green) are shown aligned to DNA-PKcs as in Figures 2A–2C. The structures are rendered using PyMOL.

## The DNA-PKcs-BRD Defines Its Activity for H2AX Phosphorylation and the Associated Cell Fate Decision

We next clarified structurally how the DNA-PKcs-BRD binding to the N-terminal K5ac facilitates phosphorylation of the C-terminal Ser139 on H2AX. Using the structure of the human nucleosome (PDB: 2CV5) as a template, we first constructed a homology model of an H2AX-containing nucleosome and then built its tail domains that are missing from the crystal structure. After manually placing the H2AX-containing nucleosome near DNA-PK, we set up constrained discrete molecular dynamics simulations (Ding et al., 2008; Dokholyan et al., 1998), which showed a possibility for simultaneous binding of Kac and Ser139 to regions corresponding to the BRD and the catalytic domain of DNA-PKcs (Figure 4). Furthermore, the highly specific recognition of N6-Kac by BRD would fulfill a structural need for stabilization of the contact between its catalytic domain and the H2AX tail; this recognition would also enable DNA-PKcs to selectively bind K5ac-H2AX and target Ser139 for phosphorylation, an event that would be lost by substitution of lysine 5 with alanine, consequently making the kinase domain of DNA-PKcs less favorable to phosphorylate Ser139. The significant structural homology indicates that the binding of DNA-PKcs-BRD to K5ac could induce a conformational change favorable for DNA-PKcs to recognize H2AX Ser139.

As an immediate validation of the K5ac docking of DNA-PKcs, we determined how H2AX K5ac affects the co-localization between H2AX as well as IR-induced DNA-PKcs activation by using the cells transfected with either FLAG-tagged WT H2AX or a non-acetylatable K5A mutant of H2AX correctly packed into chromatin (Du et al., 2006). In 10 Gy-irradiated cells, compared with the co-localized foci between more activated DNA-PKcs indicated by a DNA-PKcs activity marker, phospho-Thr2609 (Chen et al., 2007) (in red) and WT H2AX, DNA-PKcs not only weakly co-localized with the non-acetylatable H2AX mutant K5A but also became less activated in the absence of Kac (Figure S7B). Notably, little γ-Ser139 was detected on the FLAG-tagged H2AX K5A mutant from the 10 Gy-irradiated cells with a 1-hr post-IR recovery (Figure S7C), indicating that activation of DNA-PKcs requires prior acetylation at K5.

Next, to experimentally validate our modeling illustrating BRD/K5ac-dependent induction of γ-Ser139, we first studied how the exogenously expressed DNA-PKcs-BRD affects the γ-Ser139 level induced by an acute IR by transfecting U2OS cells with either plasmid of EV, the one expressing BRD4 or DNA-PKcs-BRD, or the single or triple mutant of DNA-PKcs-BRD prior to 10 Gy IR. As shown by Figures 5A and 5B, the IR-induced level of γ-Ser139 was reduced with the over-expression of either DNA-PKcs-BRD or BRD4. Furthermore, in correlation with the changes in the interaction between DNA-PKcs and H2AX, the significantly reduced level of IR-induced γ-Ser139 in the U2OS cells expressing either DNA-PKcs-BRD (even with the lowest expressed amount) or BRD4 was not observed in those over-expressing either mutant of DNA-PKcs-BRD$_{N2176A}$ or DNA-PKcs-BRD$_{P2110A/N2176A/M2185A}$ (Figure 5A), supporting our structural model that DNA-PKcs phosphorylates H2AX Ser139 in a BRD-dependent way during acute IR whereby the exogenously expressed DNA-PKcs-BRD could compete off the endogenous DNA-PKcs from the same H2AX K5ac site and, therefore, disrupt the docking of endogenous DNA-PKcs on K5ac for Ser139 phosphorylation. These loss-of-function experiments demonstrated that the specificity of the BRD of DNA-PKcs in defining its K5ac-dependent, H2AX-associated kinase activity in DDR as the DNA-PKcs-BRD structure plays a regulatory role in phosphorylating Ser139.

We next investigated how the Kac-dependent activation of DNA-PKcs affects cellular sensitivity to radiation. Along with the IR-induced level of γ-Ser139 being reduced with increasing expression of either DNA-PKcs-BRD or BRD4, we observed a decreasing amount of ubiquitinated γ-Ser139 H2AX in 10 Gy-irradiated cells transfected with EV (Figure 5B). Meanwhile, both phospho-Ser63 of c-Jun and cleaved PARP-1, the known apoptotic markers, were found to be diminished in the cells transfected by either DNA-PKcs-BRD or BRD4, indicating that by competing off the endogenous counterpart the expression of exogenous DNA-PKcs-BRD or BRD4 interferes with the

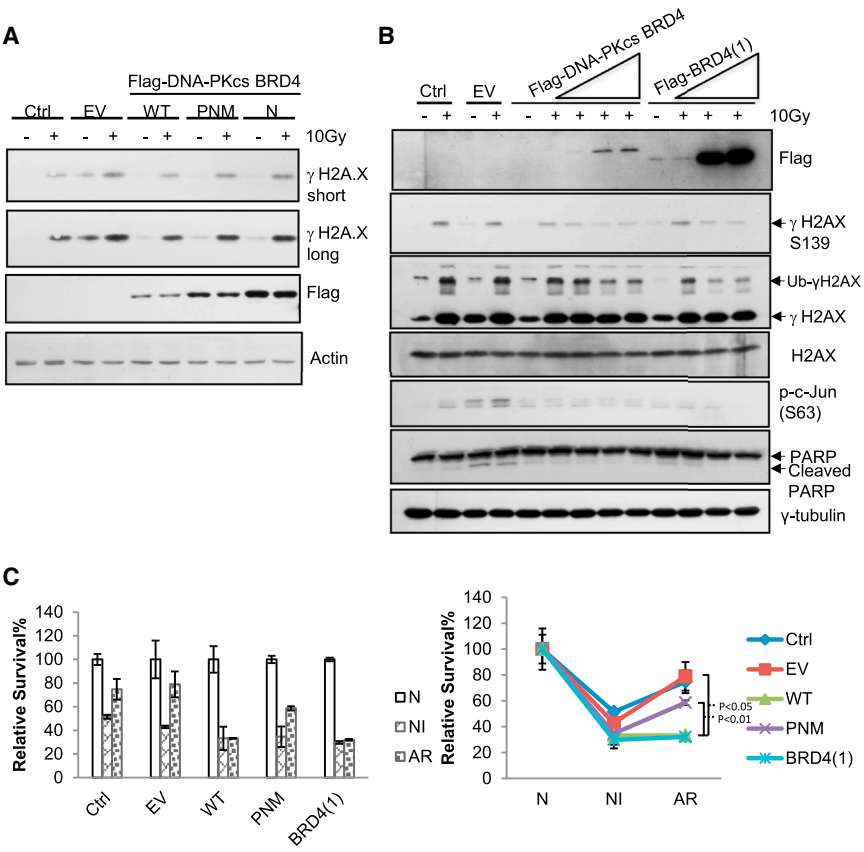


**Figure 5. The Non-canonical DNA-PKcs-BRD Defines its Kinase Activity Specifically for Phosphorylating Ser139 and the Associated Cell Fate Decision**

(A) Immunoblot analysis of the effects of the exogenously expressed (Ctrl), empty vector (EV), wild-type DNA-PKcs-BRD (WT, aa 2,070–2,200), or the mutants of single (N2176A; N) or triple (P2110A/N2176A/M2185A; PNM) site substitution(s) within the BRD of DNA-PKcs on the 10 Gy-induced level of γ-Ser139 on H2AX.

(B) Immunoblot analysis of the effects of the exogenously expressed (Ctrl), empty vector (EV), or wild-type DNA-PKcs-BRD (WT) or BRD4 on the propensity of the acute-IR-irradiated U2OS cells. Multiple apoptotic markers including phosphor-ser63 of c-Jun and cleaved PARP were assayed by the indicated antibodies.

(C) Clonogenic survival analysis of the effects of the exogenously expressed (Ctrl), empty vector (EV), wild-type DNA-PKcs-BRD (WT) or the mutants of single (N) or triple (PNM) site substitution(s) within the BRD of DNA-PKcs or BRD4 on the survival of differently irradiated cells. Following the transfection of each given vector, the U2OS cells were treated, respectively, with either non-irradiation (N), 2 Gy acute irradiation (NI), or 0.1 Gy priming for 24 hr then 2 Gy irradiation (adaptive resistance; AR).

function of the previously characterized DNA-PKcs in the acute IR-induced, H2AX-mediated apoptosis (Sakasai et al., 2010). This result further indicated that specifically in IR-responsive cells, the BRD of DNA-PKcs defines the H2AX-mediated, pro-apoptotic activity of DNA-PKcs.

## Dysregulated DNA-PKcs Activity in NHEJ Repair Is BRD/K5ac Dependent and Contributes to Cellular Resistance to Radiation

Given the regulatory role of H2AX K5ac in DNA-PKcs activation as well as the previously observed radioresistance that is associated with the early activation of DNA-PKcs (Deriano et al., 2005) we first determined whether DNA-PKcs-BRD has an impact on the fate of chronically irradiated cells. Similarly, we respectively generated various radiation-phenotypic U2OS cells showing different sensitivities to IR, including "non-irradiated (N)," 2 Gy acutely irradiated "IR-responsive (NI)," and 2 Gy-irradiated, 0.1 Gy-primed "IR-adaptive-resistance (AR)" cells (Lee et al., 2012). Furthermore, under defined IR-phenotypic conditions we comparatively analyzed the survival level of each phenotypic cell set with or without transfection of either WT or the mutant DNA-PKcs-BRD or BRD4, respectively, by using clonogenic survival assay. As shown in Figure 5C, the increased percentages of the surviving cells under AR with respect to that of the NI cells were reversed only by the exogenously expressed WT DNA-PKcs-BRD and not by the mutant of DNA-PKcs-BRD. Note that similarly low percentages of the surviving cells were observed for all cells following an acute 2 Gy IR (NI), probably due to the acute, toxic effect of over-expressed DNA-PKcs-BRD or its mutant. These results indicated that, specifically in the IR-resistant cells, the BRD of DNA-PKcs may play a pro-survival role.

Given the regulatory role of DNA-PKcs activity in NHEJ, we then investigated the impact of DNA-PKcs-BRD on its NHEJ-associated activity. First, given that the integrity of the DNA-PK complex involving other DNA end-joining components such as Ku70/80 is required for the activity of DNA-PKcs in NHEJ repair (Deriano et al., 2005), we asked whether the formation of the DNA-PKcs/Ku70 complex is mediated by the BRD-dependent H2AX code, K5ac. Accordingly, we evaluated the JQ1 effect of on the IR-induced association between H2AX and the DNA-PKcs/Ku70 complex by immunoprecipitating H2AX from the 10 Gy-irradiated cells without or with JQ1 pre-treatment. As shown in Figure 6A, the 10 Gy-induced association between H2AX and DNA-PK complex was completely disrupted in the JQ1 pre-treated cells, similar to the effect of the exogenously expressed DNA-PKcs (Figure 3D), indicating that formation of the DSB-repairing DNA-PK complex was K5ac dependent, as JQ1 competed with K5ac for binding to DNA-PKcs-BRD due to its specificity in binding BRD4 (Filippakopoulos et al., 2010), leading to destabilization of the DNA-PK complex involved in NHEJ.

We then investigated the impact of the acetyl-H2AX-dependent activation of DNA-PKcs in NHEJ repair and the associated cellular sensitivity to radiation. We first measured the time-dependent changes of DNA-PK activity in 5 Gy-irradiated

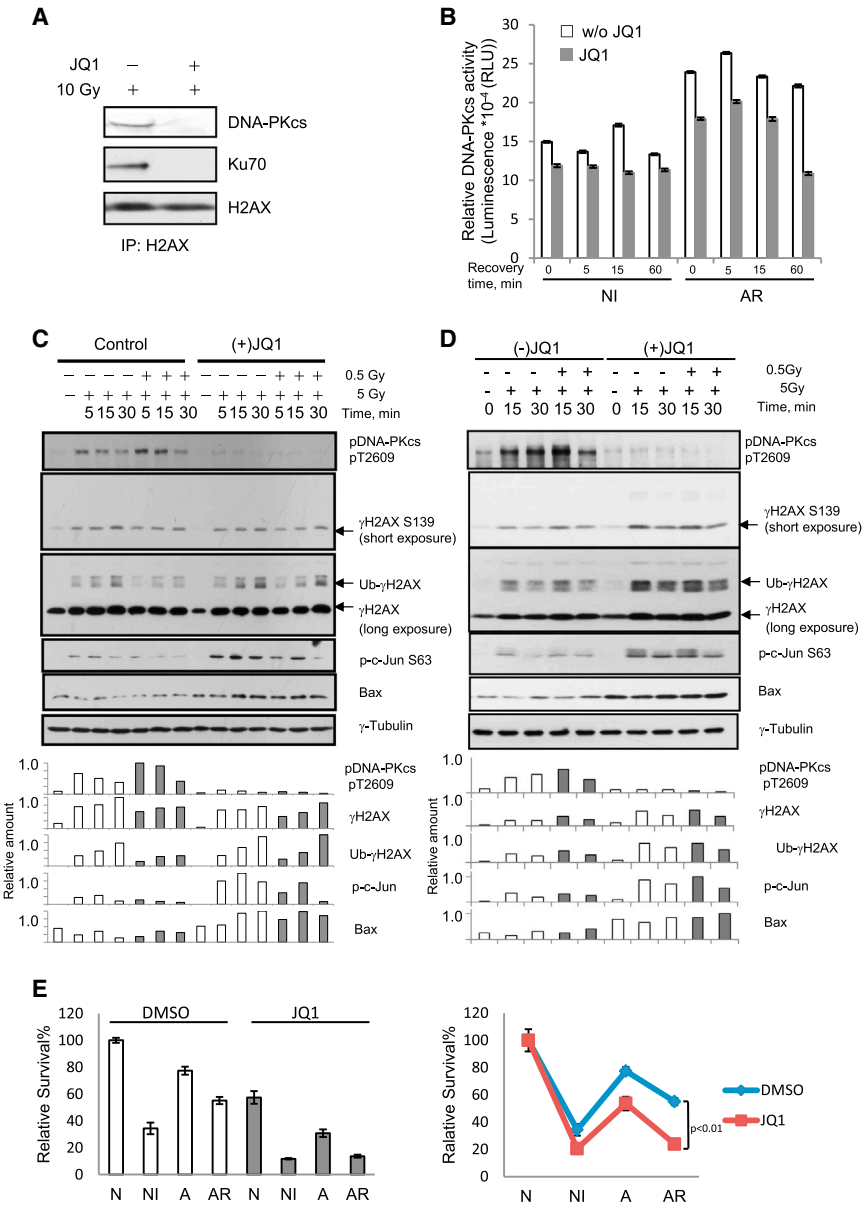


**Figure 6. IR-Induced, K5ac-Dependent Activation of DNA-PKcs Contributes to the Radioresistance of Tumor Cells, which Could Be Re-sensitized by the Active Form of (+)-JQ1**

(A) Formation of the DNA-PK complex in DSB end-repair is acetylation/BRD dependent. Immunoblot analysis of the immunoprecipitates pulled down by anti-H2AX antibody immobilized on beads from, respectively, the nuclear fractions of the 10 Gy IR-treated HeLa cells pre-treated without or with JQ1. DNA-PKcs or Ku70 was visualized with the indicated antibodies with H2AX as the loading control.

(B) Measurements of time-dependent DNA-PKcs activity in naive or low-dose IR-primed K562 leukemia cells without or with JQ1 pre-treatment using DNA-PK pull-down kinase assays. Each bar represents the mean ± SD of triplicates.

(C) JQ1 re-sensitizes radioresistant cancer cells through inhibiting the K5ac-initiated, over-active DNA-PKcs. Immunoblot analysis of time-dependent changes of DNA-PKcs-mediated NHEJ activity (indicated by pT2609) in naive or low-dose IR-primed K562 leukemia cells without or with JQ1 pre-treatment. The changes in γH2AX, ubiquitinated γH2AX, phosphor-ser63 on c-Jun, and expression of Bax were also measured. Immunoblot intensities were quantified by densitometry.

(D) Comparative effects of the active (+)-JQ1 versus the inactive (−)-JQ1 on the cellular responsiveness to radiation and the cell fate decision.

(E) Clonogenic survival analysis of the effect of (+)-JQ1 on the survival of U2OS cells under N, NI, and AR conditions.

leukemia K562 cells without or with a low-dose IR priming at 0.5 Gy, each phenotypically categorized as either NI or AR cells, respectively (Lee et al., 2012). At the early time points of post-IR recovery, DNA-PKcs was more activated in AR cells than in NI cells (Figure 6B). Furthermore, given that phosphorylation of Thr2609 on DNA-PKcs plays a critical role in the NHEJ pathway (Chen et al., 2007), the level of phospho (p)-Thr2609 should indicate the activation status of DNA-PKcs-mediated NHEJ repair. As measured with an anti-pThr2609 antibody, and similar to the change in DNA-PK activity (Figure 6B), the early activation of DNA-PKcs-mediated NHEJ repair was also observed in IR-resistant cells (Figure 6C, lanes 5, 6 versus 2, 3). Also, the expression of IR-inducible apoptotic markers pSer63 c-Jun and Bax were suppressed in AR cells along with a reduced level of ubiquitinated γ-Ser139 H2AX. These observations agree with two other reports that showed (1) similar early activation of DNA-PKcs in resistant B-cell chronic lymphocytic leukemia (Deriano et al., 2005), and (2) stimulated DDR through acetylation-dependent ubiquitination of H2AX (Ikura et al., 2007), together indicating that the over-activation of DNA-PKcs contributes to increased resistance to apoptosis and reduced sensitivity to radiation. Because compared with non-irradiated cells lysine 5 remained acetylated in the presence of prolonged IR (Figure S2B), we concluded that the early activation of DNA-PKcs in IR-resistant cells is caused by its BRD recognizing the residual K5ac maintained by priming radiation.

More importantly, these results suggest that JQ1 could be a putative sensitizer of the tumor cells with radioresistance. We therefore examined the effect of (+)-JQ1 treatment on DNA-PKcs-mediated sensitivity to IR. While DNA-PK activity and the level of pThr2609 were significantly reduced in both IR-sensitive and IR-resistant cells pre-treated with (+)-JQ1 (Figures 6B and 6C), indicating the (+)-JQ1-mediated inhibition of the K5ac-dependent activity of DNA-PKcs in NHEJ repair, both pSer63 c-Jun and Bax were more pronounced in the JQ1-treated cells under the IR-resistant condition along with an increased level of ubiquitinated γ-Ser139 H2AX (30 min after the second irradiation) (Figure 6C, lanes 12, 13 versus 6, 7,

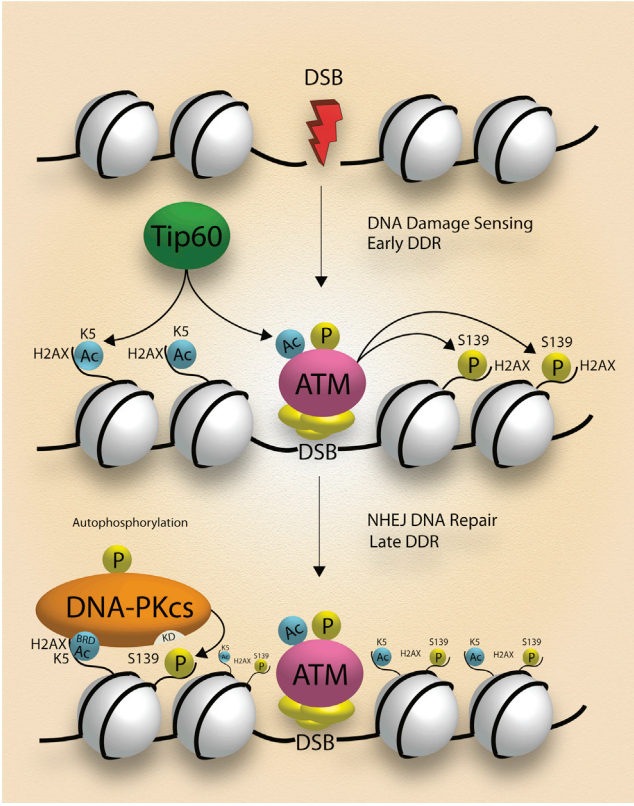


**Figure 7. Mechanistic Scheme of IR-Induced, K5ac-Dependent Activation of DNA-PKcs for H2AX Ser139 Phosphorylation**

Acute IR Tip60-mediated acetylation of K5 on H2AX facilitates the docking of DNA-PKcs that uses its BRD4-like domain to recognize K5ac. The K5ac-dependent activation of DNA-PKcs further phosphorylates H2AX Ser139. In the presence of prolonged low-dose IR, the residual K5ac is responsible for the early activation of DNA-PKcs, which promotes the H2AX-mediated radioresistance.

and lane 14 versus lane 7). Meanwhile, along with measurement of all markers of apoptosis and cell fate status already mentioned, we compared the effect of pre-treatment with the active (+)-JQ1 and its inactive counterpart (−)-JQ1. As shown in Figure 6D, similar to non-treated cells under all conditions, pre-treatment using (−)-JQ1 caused little change in the responsiveness of the radioresistant tumor cells to radiation, illustrating the specificity of the active form (+)-JQ1 in recognizing the BRD of DNA-PKcs. Also, we comparatively examined the effect of (+)-JQ1 on the survival of the cells under N, NI, and AR, whereby pre-treatment with (+)-JQ1 led to reduced survival under all different IR conditions, with a more significant reduction of AR cells (Figure 6E).

Clearly, by inhibiting the over-heated, K5ac-dependent activity of DNA-PKcs, JQ1 could offer refractory cellular resistance to radiation and restore sensitivity of IR-resistant cells to DSB-induced apoptosis. Notably, although DNA-PKcs is over-activated in IR-resistant cells, little change at the level of γH2AX was observed. This is probably due to protein phosphatase 2A (PP2Ac), which we found was constitutively activated specifically in cells in the chronic inflammatory state (Xie et al., 2013). The chronically active PP2Ac could dephosphorylate γH2AX and offset the increase of γH2AX caused by over-activated DNA-PKcs (Y.Z. et al., unpublished data).

## DISCUSSION

Our discovery of the BRD-like domain module in DNA-PKcs was supported by other recent evidence from different groups including: (1) BRD4 binding to H2A K5ac that is conserved in H2A and H2AX (Filippakopoulos et al., 2012); (2) with a DSB inducer (MNNG), ATM and DNA-PK play a sequential role in inducing γH2AX (Baritaud et al., 2012); and (3) the NHEJ pathway where DNA-PK is a major player could be the target pathway for re-sensitizing radioresistant tumors (Srivastava et al., 2012).

Prior to our findings, H2AX PTMs were individually studied, as little was found for the cooperative functions of multiple H2AX PTMs. The major technical barrier is that bottom-up MS proteomics (analysis of proteolytic digests) are capable only of identifying PTMs in MS-detectable peptides, so the connectivity among PTMs in disparate portions of a protein could be lost. Specifically for H2AX, although either γ-Ser139 (Zhu et al., 2002) or H2AFZ K5ac (Choudhary et al., 2009) was individually identified by MS, possible connectivity among these PTMs was never observed because their remote locations separate them by >130 residues. In this regard, our top-down MS sequenced the full-length H2AX, simultaneously identifying different PTM sites within both N- and C-terminal tails. Without the enrichment step essential for low-abundance PTM analysis using bottom-up approaches, all of the phosphorylated/acetylated forms of H2AX were detected by FTICR MS at good signal-to-noise (S/N) ratio, with sufficient ion intensity for ECD MS/MS sequencing. By contrast, bottom-up analysis of the same set of samples gave no confident assignments of these modified peptides (data not shown). Meanwhile, unlike a bottom-up experiment in which most PTM-containing peptides, phosphopeptides in particular, are ionized much less efficiently than their unmodified counterparts, leading to poor S/N ratio, different forms of an intact protein, either modified or unmodified, are equally ionized because either single or multiple PTM sites have little effect on the overall ionization efficiency of their parent proteins. As a result, relative intensities of the FTICR MS signals derived from either unmodified or modified H2AX were proportional to their relative abundances.

Mechanistically we have revealed that, due to the unique BRD structure found only in DNA-PKcs, ATM and DNA-PK play the timing roles in H2AX phosphorylation during DDR: ATM is more involved in the γH2AX-mediated DSB recognition, whereas in a K5ac-dependent manner DNA-PKcs is more active in the γH2AX-mediated DNA repair or apoptosis of irreparable cells. Given that DSBs rapidly induce the Tip60-mediated acetylation of ATM for initiating its activity (Sun et al., 2007), the activated ATM therefore could immediately target H2AX Ser139 in a K5ac-independent way prior to the activation of DNA-PKcs. In parallel with the function of the K5ac depositor Tip60 in selective histone variant exchange at DNA lesions (Kusch et al., 2004), the timely K5ac-mediated docking of DNA-PKcs on H2AX promotes H2AX-mediated DSB repair (Figure 7).

Notably, in the IR phenotype-specific manner, this non-canonical BRD module in DNA-PKcs induces γH2AX and promotes apoptosis of acutely irradiated cells; in IR-responsive cells,

introduction of an exogenous DNA-PKcs-BRD or BRD4 attenuates H2AX phosphorylation, whereas expression of the DNA-PKcs constructs harboring mutations that abrogate key residues in DNA-PKcs-BRD had little effect on the γH2AX level (Figures 5A and 5B). This finding agrees with a reported role of BRD4 in inhibiting the radiation-induced γH2AX (Floyd et al., 2013). The level of γH2AX showed little change or a slight decrease in the radiation-responsive cells that were pre-treated with (+)-JQ1, whereas JQ1 treatment of the radiation-resistant cells led to increased levels of Ub-γH2AX (Figures 6C and 6D). This novel finding reveals that there is a differential effect of JQ1 depending upon either the radiation-responsive or radiation-resistant nature of the cancer cells: JQ1 inhibits only radiation-induced H2AX signaling in the radiation-responsive/-sensitive cells and, conversely, JQ1 sensitizes the resistant cells through interrupting the DNA-PK BRD-mediated mechanism.

Although DNA-PKcs is a crucial enzyme in proper NHEJ repair, in a variety of carcinomas DNA-PKcs has been found not only to be over-expressed but also correlated with dysregulated NHEJ for radioresistance. A 2012 report indicated that the therapeutic resistance of tumor cells could be overcome by the inhibition of NHEJ through interfering with the DNA-binding domain of ligase IV (Srivastava et al., 2012). Here, we showed that the DNA-PKcs-BRD4-interfered or JQ1-mediated inhibition of the dysregulated, NHEJ-specific activity of DNA-PKcs led to the activation of intrinsic apoptotic pathways and the re-sensitization of radioresistant tumor cells similar to those induced by a ligase IV-targeting molecule SCR7, suggesting that the NHEJ pathway is a reservoir of new drug targets for overcoming therapeutic resistance.

In summary, we reveal the mechanism by which a DDR-phenotypic pattern of PTMs, including γH2AX, is sequentially established on H2AX, and how these H2AX PTMs affect in turn the activities of specific enzyme(s) involved in the H2AX-coordinated DDR and the corresponding cell fate decision. Although the precise mechanism underlying how over-activated, DNA-PKcs-mediated NHEJ repair inhibits apoptotic pathways remains to be further elucidated, we show the BRD4-like domain of DNA-PKcs to be a modulator of the acetylation-dependent NHEJ activity of DNA-PKcs. Because we revealed a novel intervention target of a non-catalytic BRD domain of DNA-PKcs that differs from its kinase catalytic domain at which most conventional DNA-PKcs drugs are targeted, co-administration of JQ1 with a selected existing drug may represent a combination therapy strategy to increase the specificity and effectiveness of NHEJ-targeting treatments of cancer.

## SIGNIFICANCE

**Cells constantly exposed to IR may acquire radioresistance. Through an unknown mechanism this adaptive effect, if dysregulated, contributes to an increased risk of carcinogenesis. Here we discover a bromodomain (BRD)-like module in the catalytic subunit of DNA-PKcs or DNA-PKcs-BRD that specifically recognizes H2AX K5ac for sequential induction of phosphorylation of γH2AX, an immediate indicator of DNA damage. Although diverse BRD families are found in different nuclear proteins including acetylases, ATP-dependent chromatin-remodeling complexes, helicases, methyltransferases, and transcriptional activators/mediators, until now there has been no report of the presence of BRD(s) in a protein kinase directly functioning in chromatin-associated DSB recognition/repair. Our combined approaches of top-down MS, sequence-structure modeling/docking, site-directed mutagenesis, and biochemical experiments illustrated that, through docking on H2AX K5ac, this non-canonical BRD determines not only the H2AX-targeting activity of DNA-PKcs but also the over-activation of DNA-PKcs in radioresistant tumor cells, whereas a Kac antagonist JQ1 was able to bind to DNA-PKcs-BRD, leading to re-sensitization of tumor cells to radiation. To our knowledge, this is the first report of a BRD occurring in a DNA repair protein that acts as both reader and writer of distinct histone codes for H2AX-mediated cell fate decision. Furthermore, our discovery explains the nucleosome/chromatin dependence of activation of DNA repair enzyme(s) and exactly how the active DNA-PK complex accesses damaged DNA in chromatin. We therefore reveal a new, Kac-dependent mechanism underlying the activation of DNA-PKcs wherein the DSB-inducible K5ac on H2AX is identified as a new epigenetic code to define the H2AX-mediated DDR and the associated cell fate decision.**

## EXPERIMENTAL PROCEDURES

### Cells, Reagents, and Antibodies

HEK 293T, HeLa, and U-2 OS cell lines were from the American Type Culture Collection. Human glioma cell lines M059K and M059J were a gift from the laboratory of Dr. Aziz Sancar. Cells were maintained respectively in either DMEM, RPMI-1640, or McCoy's 5a medium (Invitrogen). JQ1 (Structural Genomics Consortium) was re-suspended in DMSO to a final concentration of 5 mM. The Superfect transfection reagent was from Qiagen. Antibodies for DNA-PKcs, phospho-ser63 c-Jun, and Bax were from Cell Signaling. Antibodies of Tip60 and γTyr142H2AX were from Millipore. Antibodies for γH2AX (S139, ab22551), H2A K5ac (ab45152), H2AX (ab11175), and DNA-PKcs pT2609 (ab4194) were from Abcam. FLAG M2 was from Sigma. DNA-PKcs pT2609 for immunoblotting was a gift from Dr. Dale Ramsden. DNA-PKcs peptide substrate and Kinase-Glo Plus Luminescent Kinase Assay kit were from Promega.

### Cell Irradiation

Cells were grown to 60%–70% confluence before IR. A γ-ray source (AECL Gammacell 40 Irradiator) irradiates cells at defined doses or for different lengths of time at a dose rate of 1 Gy/min. After IR, the cells were allowed to recover for a defined time and washed with PBS for further analysis.

### Purification of Full-Length Histone H2AX for Top-Down MS

A Histone Purification Mini Kit (Active Motif) was used for histone extraction in the presence of protease (Roche Diagnostics) and phosphatase inhibitor cocktails (Sigma-Aldrich). Following acetone precipitation the resulting pellet containing histones was air-dried thoroughly, and suspended in $H_2O$. 50 μg of histones was purified by RP HPLC with a ZORBAX C8 column (4.6 × 150 mm, 5 μm particle sizes). With solvent A (water pre-mixed with 0.1% trifluoroacetic acid [TFA]) and solvent B (acetonitrile pre-mixed with 0.1% TFA) core histones were eluted by using a multi-step gradient with 0%–5% B for 10 min, 5%–24% B for 10 min, 25%–64% B for 80 min, 65%–99% B for 20 min, and isocratic gradient for 20 min at 100% with a flow rate of 200 μl/min. MS spectra were acquired by a hybrid Qe-FTICR MS, equipped with a 12.0-T magnet (Apex 12.0 T AS, Bruker Daltonics) and an Apollo II microelectrospray ionization source. MS raw data acquired from ApexControl (version 2.0, build 36) were processed using DataAnalysis 3.4 Build 191 software.

### Measurements of Binding between DNA-PKcs-BRD and JQ1 or H2AX Peptides

The JQ1-Sepharose or empty beads blocked by 3 mg/ml BSA in PBS were incubated with the freshly re-folded DNA-PKcs-BRD in a buffer containing 20 mM Tris (pH 8.0), 150 mM NaCl, 1 mM EDTA, 1% CA630, and 1 mg/ml BSA for 2 hr, and washed with the same buffer three times before elution with SDS sample buffer. For the comparative studies of peptide binding and JQ1 competition, the method of Fuchs et al. (2010) with minor modifications was used. 2 μg of WT H2AX peptide with the sequence SGRGKTGGKARA KAKSR-Peg-Biotin or the H2AX K5ac-containing peptide counterpart was incubated with streptavidin beads for 1 hr at 4°C and then washed twice with a peptide binding buffer (PBB; 50 mM Tris [pH 8.0], 300 mM NaCl, 0.1% NP-40). The freshly re-folded protein (80 pmol) was incubated with each of the peptides on beads at 4°C overnight and then washed three times with PBB. The DNA-PKcs-peptide complexes were eluted with 1× SDS gel sample buffer, separated in a NuPAGE 3%–8% Tris-acetate gel (Invitrogen), and analyzed by immunoblotting against anti-His or anti-GST antibody. For JQ1 competition experiments, 10 μM JQ1 was added.

### JQ1 Treatment of K562 Cells

Prior to irradiation, K562 cells were pre-treated with 500 nM (+)-JQ1 or (−)-JQ1 from a 5-mM stock in DMSO for 24 hr.

## SUPPLEMENTAL INFORMATION

Supplemental Information includes Supplemental Experimental Procedures, three tables, and seven figures and can be found with this article online at http://dx.doi.org/10.1016/j.chembiol.2015.05.014.

## AUTHOR CONTRIBUTIONS

L.W., L.X., and Y.L. performed sample preparation including H2AX purification, cell culture, site-directed mutagenesis, and biochemical/immunoblot assays. L.Z. collected and analyzed the top-down MS data using FTICR. S.R. and N.V.D. performed modeling analysis. C.Z. performed circular dichroism. J.J. and F.L. synthesized and provided immobilized JQ1. B.D.S and K.K. synthesized the H2AX peptides. X.C. conceived the project, designed the experiments, analyzed the data, and wrote the manuscript. All authors discussed the results and commented on the manuscript.

## ACKNOWLEDGMENTS

This work is primarily supported in part by multiple grants to X.C. including Chinese 973 fund 2013CB910802, US NIH 1U24CA160035 from the National Cancer Institute Clinical Proteomic Tumor Analysis Consortium (CPTAC), and NIAID 1U19AI109965, and was also supported by NIH R01GM103893 (to J.J.), R01GM080742 (to N.V.D.), and R01CA162804 and R01CA92584 (to D.J.C). We thank William K. Kaufmann for providing ATM/mutant cell lines, and Dale A. Ramsden for suggestions. We are grateful to Dr. James E. Bradner for providing JQ1 and Dr. Howard Fried for proofreading the manuscript.

Received: January 26, 2015
Revised: May 12, 2015
Accepted: May 14, 2015
Published: June 25, 2015

## REFERENCES

Baritaud, M., Cabon, L., Delavallee, L., Galan-Malo, P., Gilles, M.E., Brunelle-Navas, M.N., and Susin, S.A. (2012). AIF-mediated caspase-independent necroptosis requires ATM and DNA-PK-induced histone H2AX Ser139 phosphorylation. Cell Death Dis. *3*, e390.

Berman, H.M., Westbrook, J., Feng, Z., Gilliland, G., Bhat, T.N., Weissig, H., Shindyalov, I.N., and Bourne, P.E. (2000). The Protein Data Bank. Nucleic Acids Res. *28*, 235–242.

Bonner, W.M., Redon, C.E., Dickey, J.S., Nakamura, A.J., Sedelnikova, O.A., Solier, S., and Pommier, Y. (2008). γH2AX and cancer. Nat. Rev. Cancer *8*, 957–967.

Bruce, I., Akhlaq, M., Bloomfield, G.C., Budd, E., Cox, B., Cuenoud, B., Finan, P., Gedeck, P., Hatto, J., Hayler, J.F., et al. (2012). Development of isoform selective PI3-kinase inhibitors as pharmacological tools for elucidating the PI3K pathway. Bioorg. Med. Chem. Lett. *22*, 5445–5450.

Chen, B.P., Uematsu, N., Kobayashi, J., Lerenthal, Y., Krempler, A., Yajima, H., Lobrich, M., Shiloh, Y., and Chen, D.J. (2007). Ataxia telangiectasia mutated (ATM) is essential for DNA-PKcs phosphorylations at the Thr-2609 cluster upon DNA double strand break. J. Biol. Chem. *282*, 6582–6587.

Choudhary, C., Kumar, C., Gnad, F., Nielsen, M.L., Rehman, M., Walther, T.C., Olsen, J.V., and Mann, M. (2009). Lysine acetylation targets protein complexes and co-regulates major cellular functions. Science *325*, 834–840.

Cook, P.J., Ju, B.G., Telese, F., Wang, X., Glass, C.K., and Rosenfeld, M.G. (2009). Tyrosine dephosphorylation of H2AX modulates apoptosis and survival decisions. Nature *458*, 591–596.

Deriano, L., Guipaud, O., Merle-Beral, H., Binet, J.L., Ricoul, M., Potocki-Veronese, G., Favaudon, V., Maciorowski, Z., Muller, C., Salles, B., et al. (2005). Human chronic lymphocytic leukemia B cells can escape DNA damage-induced apoptosis through the nonhomologous end-joining DNA repair pathway. Blood *105*, 4776–4783.

Ding, F., Tsao, D., Nie, H., and Dokholyan, N.V. (2008). Ab initio folding of proteins with all-atom discrete molecular dynamics. Structure *16*, 1010–1018.

Ding, F., Yin, S., and Dokholyan, N.V. (2010). Rapid flexible docking using a stochastic rotamer library of ligands. J. Chem. Inf. Model. *50*, 1623–1632.

Dokholyan, N.V., Buldyrev, S.V., Stanley, H.E., and Shakhnovich, E.I. (1998). Discrete molecular dynamics studies of the folding of a protein-like model. Fold. Des. *3*, 577–587.

Du, Y.C., Gu, S., Zhou, J., Wang, T., Cai, H., Macinnes, M.A., Bradbury, E.M., and Chen, X. (2006). The dynamic alterations of H2AX complex during DNA repair detected by a proteomic approach reveal the critical roles of Ca(2+)/calmodulin in the ionizing radiation-induced cell cycle arrest. Mol. Cell. Proteomics *5*, 1033–1044.

Fang, T.C., Schaefer, U., Mecklenbrauker, I., Stienen, A., Dewell, S., Chen, M.S., Rioja, I., Parravicini, V., Prinjha, R.K., Chandwani, R., et al. (2012). Histone H3 lysine 9 di-methylation as an epigenetic signature of the interferon response. J. Exp. Med. *209*, 661–669.

Filippakopoulos, P., Qi, J., Picaud, S., Shen, Y., Smith, W.B., Fedorov, O., Morse, E.M., Keates, T., Hickman, T.T., Felletar, I., et al. (2010). Selective inhibition of BET bromodomains. Nature *468*, 1067–1073.

Filippakopoulos, P., Picaud, S., Mangos, M., Keates, T., Lambert, J.P., Barsyte-Lovejoy, D., Felletar, I., Volkmer, R., Muller, S., Pawson, T., et al. (2012). Histone recognition and large-scale structural analysis of the human bromodomain family. Cell *149*, 214–231.

Floyd, S.R., Pacold, M.E., Huang, Q., Clarke, S.M., Lam, F.C., Cannell, I.G., Bryson, B.D., Rameseder, J., Lee, M.J., Blake, E.J., et al. (2013). The bromodomain protein Brd4 insulates chromatin from DNA damage signalling. Nature *498*, 246–250.

Fuchs, S.M., Krajewski, K., Baker, R.W., Miller, V.L., and Strahl, B.D. (2010). Influence of combinatorial histone modifications on antibody and effector protein recognition. Curr. Biol. *21*, 53–58.

Heffernan, T.P., Simpson, D.A., Frank, A.R., Heinloth, A.N., Paules, R.S., Cordeiro-Stone, M., and Kaufmann, W.K. (2002). An ATR- and Chk1-dependent S checkpoint inhibits replicon initiation following UVC-induced DNA damage. Mol. Cell. Biol. *22*, 8552–8561.

Heo, K., Kim, H., Choi, S.H., Choi, J., Kim, K., Gu, J., Lieber, M.R., Yang, A.S., and An, W. (2008). FACT-mediated exchange of histone variant H2AX regulated by phosphorylation of H2AX and ADP-ribosylation of Spt16. Mol. Cell *30*, 86–97.

Holm, L., and Rosenstrom, P. (2010). Dali server: conservation mapping in 3D. Nucleic Acids Res. *38*, W545–W549.

Ikura, T., Tashiro, S., Kakino, A., Shima, H., Jacob, N., Amunugama, R., Yoder, K., Izumi, S., Kuraoka, I., Tanaka, K., et al. (2007). DNA damage-dependent

 

acetylation and ubiquitination of H2AX enhances chromatin dynamics. Mol. Cell. Biol. *27*, 7028–7040.

Kusch, T., Florens, L., Macdonald, W.H., Swanson, S.K., Glaser, R.L., Yates, J.R., 3rd, Abmayr, S.M., Washburn, M.P., and Workman, J.L. (2004). Acetylation by Tip60 is required for selective histone variant exchange at DNA lesions. Science *306*, 2084–2087.

Lee, Y.Y., Yu, Y.B., Gunawardena, H.P., Xie, L., and Chen, X. (2012). BCLAF1 is a radiation-induced H2AX-interacting partner involved in gammaH2AX-mediated regulation of apoptosis and DNA repair. Cell Death Dis. *3*, e359.

Lees-Miller, S.P., Godbout, R., Chan, D.W., Weinfeld, M., Day, R.S., Barron, G.M., and Allalunis-Turner, J. (1995). Absence of p350 subunit of DNA-activated protein kinase from a radiosensitive human cell line. Science *267*, 1183–1185.

Lobrich, M., and Jeggo, P.A. (2007). The impact of a negligent G2/M checkpoint on genomic instability and cancer induction. Nat. Rev. Cancer *7*, 861–869.

Mullenders, L., Atkinson, M., Paretzke, H., Sabatier, L., and Bouffler, S. (2009). Assessing cancer risks of low-dose radiation. Nat. Rev. *9*, 596–604.

Owen, D.J., Ornaghi, P., Yang, J.C., Lowe, N., Evans, P.R., Ballario, P., Neuhaus, D., Filetici, P., and Travers, A.A. (2000). The structural basis for the recognition of acetylated histone H4 by the bromodomain of histone acetyltransferase gcn5p. EMBO J. *19*, 6141–6149.

Park, E.J., Chan, D.W., Park, J.H., Oettinger, M.A., and Kwon, J. (2003). DNA-PK is activated by nucleosomes and phosphorylates H2AX within the nucleosomes in an acetylation-dependent manner. Nucleic Acids Res. *31*, 6819–6827.

Sakasai, R., Teraoka, H., Takagi, M., and Tibbetts, R.S. (2010). Transcription-dependent activation of ataxia telangiectasia mutated prevents DNA-dependent protein kinase-mediated cell death in response to topoisomerase I poison. J. Biol. Chem. *285*, 15201–15208.

Sibanda, B.L., Chirgadze, D.Y., and Blundell, T.L. (2010). Crystal structure of DNA-PKcs reveals a large open-ring cradle comprised of HEAT repeats. Nature *463*, 118–121.

Srivastava, M., Nambiar, M., Sharma, S., Karki, S.S., Goldsmith, G., Hegde, M., Kumar, S., Pandey, M., Singh, R.K., Ray, P., et al. (2012). An inhibitor of nonhomologous end-joining abrogates double-strand break repair and impedes cancer progression. Cell *151*, 1474–1487.

Sun, Y., Xu, Y., Roy, K., and Price, B.D. (2007). DNA damage-induced acetylation of lysine 3016 of ATM activates ATM kinase activity. Mol. Cell. Biol. *27*, 8502–8509.

van Attikum, H., and Gasser, S.M. (2009). Crosstalk between histone modifications during the DNA damage response. Trends Cell Biol. *19*, 207–217.

Wriggers, W. (2009). Using Situs for the integration of multi-resolution structures. Biophys. Rev. *2*, 21–27.

Xie, A., Odate, S., Chandramouly, G., and Scully, R. (2010). H2AX post-translational modifications in the ionizing radiation response and homologous recombination. Cell Cycle *9*, 3602–3610.

Xie, L., Liu, C., Wang, L., Gunawardena, H.P., Yu, Y., Du, R., Taxman, D.J., Dai, P., Yan, Z., Yu, J., et al. (2013). Protein phosphatase 2A catalytic subunit alpha plays a MyD88-dependent, central role in the gene-specific regulation of endotoxin tolerance. Cell Rep. *3*, 678–688.

Zhao, S., Xu, W., Jiang, W., Yu, W., Lin, Y., Zhang, T., Yao, J., Zhou, L., Zeng, Y., Li, H., et al. (2010). Regulation of cellular metabolism by protein lysine acetylation. Science *327*, 1000–1004.

Zhu, H., Hunter, T.C., Pan, S., Yau, P.M., Bradbury, E.M., and Chen, X. (2002). Residue-specific mass signatures for the efficient detection of protein modifications by mass spectrometry. Anal. Chem. *74*, 1687–1694.